RSC Advances

PAPER

View Article Online
View Journal | View Issue

Cite this: *RSC Adv.*, 2024, **14**, 4179

The radical scavenging activity of monocaffeoylquinic acids: the role of neighboring hydroxyl groups and pH levels†

Quan V. Vo, *[a] Duong Thi Thuy Hoa,[b] Nguyen Thi Hoa,[a] Manh Duc Tran[b] and Adam Mechler [c]

Caffeoylquinic acids (**CQAs**) are well-known antioxidants. However, a key aspect of their radical scavenging activity – the mechanism of action – has not been addressed in detail thus far. Here we report on a computational study of the mechanism of activity of **CQAs** in scavenging hydroperoxyl radicals. In water at physiological pH, the **CQAs** demonstrated ≈ 10^4 times higher HOO$^\bullet$ antiradical activity than in lipid medium ($k_{(lipid)} \approx 10^4$ M^{-1} s^{-1}). The activity in the aqueous solution was determined by the hydrogen transfer mechanism of the adjacent hydroxyl group (O6′–H) of the dianion states (Γ = 93.2–95.2%), while the single electron transfer reaction of these species contributed 4.8–6.8% to the total rate constants. The kinetics estimated by the calculations are consistent with experimental findings in water (pH = 7.5), yielding a $k_{calculated}/k_{experimental}$ = 2.4, reinforcing the reliability and precision of the computational method and demonstrating its utility for evaluating radical reactions *in silico*. The results also revealed the pH dependence of the HOO$^\bullet$ scavenging activity of the **CQAs**; activity was comparable for all compounds below pH 3, however at higher pH values **5CQA** reacted with the HOO$^\bullet$ with lower activity than **3CQA** or **4CQA**. It was also found that **CQAs** are less active than Trolox below pH 4.7, however over pH 5.0 they showed higher activity than the reference. The **CQAs** had the best HOO$^\bullet$ antiradical activity at pH values between 5.0 and 8.6. Therefore, in the physiological environment, the hydroperoxyl antiradical capacity of **CQAs** exhibits similarity to renowned natural antioxidants including resveratrol, ascorbic acid, and Trolox.

Received 11th December 2023
Accepted 23rd January 2024

DOI: 10.1039/d3ra08460d

rsc.li/rsc-advances

1. Introduction

Caffeoylquinic acids (**CQAs**) are a class of bioactive metabolites that are synthesized through the phenylpropanoid biosynthesis pathway.[1] These compounds are esters formed by the conjugation of caffeic acid and quinic acid. **CQAs** are frequently found in a diverse array of food sources, encompassing fruits, coffee, vegetables, spices, and an extensive variety of plant species.[2,3] **CQAs** have a diverse array of potential therapeutic uses in humans. It has been reported in a range of studies that these compounds possess antibacterial, anticancer, antiviral, anti-Alzheimer's, neuroprotective, and antioxidant properties.[1,4–14] The most common **CQA** in the plant kingdom is 5-*O*-caffeoylquinic acid (**5CQA**), also known as chlorogenic acid. This compound is usually found in combination with 3-*O*-caffeoylquinic acid (**3CQA**), also known as neochlorogenic acid, and 4-*O*-caffeoylquinic acid (**4CQA**), also known as cryptochlorogenic acid (Fig. 1).[15]

Chlorogenic acids have the ability to scavenge free radicals from a variety of sources, including 2,21-azino-bis(3-ethylbenzothiazoline-6-sulphonic acid) (ABTS) radicals, 1,1-diphenyl-2-picrylhydrazyl (DPPH) radicals, superoxide anions (O2), hydroxyl radicals (OH) and peroxynitrite (ONOO).[13,16,17] Kinetics of **5CQA** were determined experimentally: it reacts with the superoxide, peroxynitrite, and peroxyl radical with second-order kinetics and rate constants of 3.34 × 10^9, 9.60 × 10^5, 1.6 × 10^5 and 1.28 × 10^5 M^{-1} s^{-1}, respectively,[17] whereas the **5CQA** reacted with HO$^\bullet$ radicals with rate constant of 10^9–10^{10} M^{-1} s^{-1}.[18,19] Computational approaches were also used to evaluate the antioxidant activity of **CQAs**,[18–23] however the mechanism and kinetics of the HOO$^\bullet$ radical scavenging activity, especially in physiological environments and at different pH values have not been thoroughly investigated. In particular, the effect of different pH levels on the kinetics and mechanism of the radical scavenging activity of phenolic acids is well known,[24–26] and thus a more comprehensive examination is desirable. Furthermore, the examination of radical reactions

[a]*The University of Danang – University of Technology and Education, Danang 550000, Vietnam. E-mail: vvquan@ute.udn.vn*

[b]*The University of Danang – University of Sciences and Education, Danang 550000, Vietnam*

[c]*Department of Biochemistry and Chemistry, La Trobe University, Victoria 3086, Australia*

† Electronic supplementary information (ESI) available. See DOI: https://doi.org/10.1039/d3ra08460d

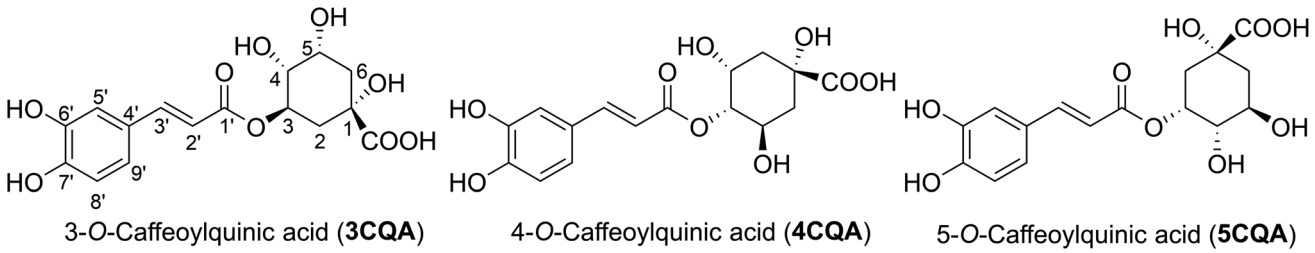

Fig. 1 Monocaffeoylquinic acids (CQAs).

involving HO$^{\bullet}$ and HOO$^{\bullet}$ is significant not only in the advanced oxidation processes,[27–29] but also in the radical scavenging activity of antioxidants.[30–33] Accordingly, in this study, thermodynamic and kinetic calculations were used to examine the hydroperoxyl radical scavenging activity of the **CQA**s in physiological conditions and at varied pH levels.

2. Computational details

The thermochemical characteristics (bond dissociation energies (BDEs), ionization energies (IEs), and proton affinities (PAs)) of the compound were investigated at the M06-2X/6-311++G(d,p) level of theory. Additionally, the kinetic parameters of the compound, including their activation energies ($\Delta G^{\neq}$) in kcal mol^{-1}, tunneling corrections (κ), and rate constants (k), were computed. The activities of the compounds were modelled in the gas phase, the physiological environment (the lipid medium consisted of pentyl ethanoate). In comparison to other intricate procedures, such as G3(MP2)-RAD, and empirical data, it has been demonstrated that the M06-2X/6-311++G(d,p) method has appropriate accuracy in the computation of thermodynamic properties, with an acceptable margin of error[34–38] and overall low error rates (k_{calc}/k_{exp} ratio = 0.3–2.9).[39–42] The kinetic calculations were conducted following the established technique for the quantum mechanics-based assay designed to evaluate the overall free radical scavenging activity (QM-ORSA) with the solvation model based on the density (SMD) method for pentyl ethanoate and water solvents. The aforementioned test has been widely employed in order to assess the antiradical properties of antioxidants.[34,35,39,40,43]

The rate constant (k) was determined through the application of the usual transition state theory (TST) under the conditions of a 1 M standard state,[44–48] and the details are shown in Table S1, ESI.†

$$k = \sigma\kappa \frac{k_B T}{h} e^{-(\Delta G^{\neq})/RT} \quad (1)$$

Here $\Delta G^{\neq}$ represents the Gibbs free energy of activation, h denotes the Planck constant, k_B represents the Boltzmann constant, s is the reaction symmetry number,[49,50] and κ signifies the tunneling corrections that were determined by the utilization of the Eckart barrier calculation method,.[51]

The computations were performed utilizing the Gaussian 16 suite of programs[52] and the Eyringpy code, depending on the particular circumstance.[53,54] Atom-in-molecule (AIM) analysis[55] was performed by using the AIM2000 software.[56]

3. Results and discussion

3.1. The thermodynamic study

Based on the core structure of **CQA**, the hexagon rings, HO, and COOH groups can undergo rotation to yield a variety of conformers. The most likely conformer to participate in a radical scavenging reaction is the most stable one, and thus electron energy levels of all possible conformers of each **CQA** were evaluated in the first stage.[57] Subsequently, the five conformers with the lowest electronic energy were subjected to free energy analysis using the M06-2X/6-311++G (d,p) level of theory. Details are shown in the ESI (Fig. S2).† It was found that the $\Delta G°$ value of **3CQA** (*i.e.* the structure as drawn in Fig. S2, ESI†) was determined to be the lowest among all the **3CQA** conformers (**3CQA-1–4**) by 2.8–5.1 kcal mol^{-1}. Similarly, the lowest energy **4CQA** and **5CQA** conformers are drawn in Fig. S2, ESI.† The estimation of conformer relative populations using the Maxwell–Boltzmann distribution[58,59] revealed that the conformers **3CQA**, **4CQA**, and **5CQA** dominate the populations (>95%) under standard conditions; consequently, these conformers were used in subsequent investigations.

In order to evaluate the likelihood of reacting with free radicals of all possible X–H (X = C, O) bonds including C–H (C2, C3, C4, C5 and C6), and O–H (COOH, O1, O3, O5, O6′ and O7′, Fig. 1) key thermochemical characteristics: bond dissociation energies (BDEs), proton affinities (PAs), and ionization energies (IEs) that provide a first approximation for the probability of reactions following either of the three respective mechanisms, *i.e.* FHT (formal hydrogen transfer), SET (single electron transfer) and PL (proton loss),[41,60,61] were first computed in physiological environments (and water (W) and pentyl ethanoate (P)). The results are shown in Fig. 2.

The lowest BDE values were observed at the O6′(7′)–H bonds in all of the studied acids with BDE(O6′(7′)–H) = 79.1–81.9 kcal mol^{-1} for the lipid medium and BDE(O6′(7′)–H) = 82.7–85.4 kcal mol^{-1} for the aqueous solution (Fig. 2a1–c1). The active site can be attributed in all cases to the formation of intramolecular hydrogen bonds between the hydrogen atoms of the adjacent hydroxyl groups and the O6′(O7′) radicals.[60,62] While the values for other O–H bonds ranged from 104.9 to 131.6 kcal mol^{-1}, the BDE(C–H) values were between 88.3 and 102.6 kcal mol^{-1}. Surprisingly the H-abstraction of the COO–H

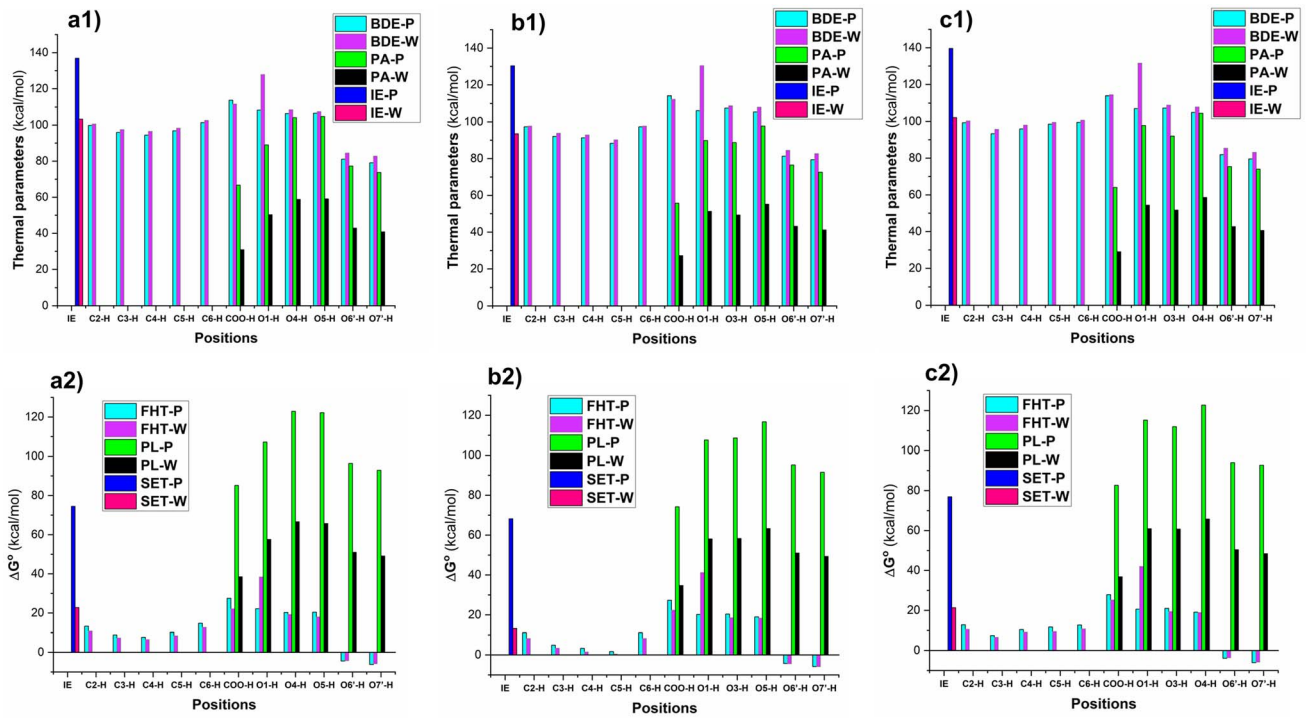

Fig. 2 The computed BDE, PA, IE (kcal mol^{-1}) of **CQAs** and $\Delta G°$ (kcal mol^{-1}) of the HOO$^{\bullet}$ + **CQAs** reactions following the SET, PL, and FHT mechanisms (a: **3CQA**; b: **4CQA**; c: **5CQA**).

bond was less likely with the BDE(COO–H) = 112.3–114.4 kcal mol^{-1} (to emphasize, this refers to hydrogen abstraction; proton dissociation is much more likely, see below). The BDE values in the water were slightly higher than those in the pentyl ethanoate solvent. As expected the PA and IE values in the polar medium were lower than those of the nonpolar environment. The deprotonation was in the order of COO–H > O7′–H > O6′–H in all of the studied compounds, whereas the IE values varied from 93.5 to 139.6 kcal mol^{-1}.

The evaluation in the Gibbs free energies ($\Delta G°$, Fig. 2a2–c2) of the HOO$^{\bullet}$ + **CQAs** reactions following either of the three pathways revealed that the HOO$^{\bullet}$ radical trapping activity of **CQAs** is only spontaneous *via* the hydrogen transfer of the O6′(7′)-H bonds ($\Delta G° = -3.6$ to -6.2 kcal mol^{-1}), whereas the other FHT reactions cannot happen in the studied media due to the positive $\Delta G°$ values. The SET mechanism is not spontaneous either in any of the studied environments, thus this reaction of the neutral states of **CQAs** can be safely ignored in the kinetic study. It is important to notice that the PL reactions are not spontaneous either in any of the studied environments; however, the PA values were substantially lower than the corresponding BDE values, thus the deprotonation of **CQAs** should be considered in the aqueous solution. Previous studies indicated that the addition reaction into the α,β-unsaturated bond had no contributions to the ROO$^{\bullet}$ radical (*i.e.*, HOO$^{\bullet}$ and $CH_3OO^{\bullet}$) scavenging activity, particularly in the physiological environments,[19,24,63] and RAF reaction is not supported for the π system of aromatic rings.[64,65] Thus, this reaction was omitted in our study. Hence, in the lipid medium, the H-abstraction of the O6′(7′)–H bonds should be used to compute rate constants, whereas, in the aqueous solution, proton dissociation should be assessed before the kinetic investigation.

3.2. The kinetics of antioxidant activity

3.2.1. The deprotonation of CQA. The dissociated form of acidic species frequently overshadows the antiradical activity of the neutral species in aqueous environments.[37,41] Thus the protonation states of **CQAs** in water at the physiological pH were analyzed. The structure of **CQAs** permits protonation at the COOH (pK_{a1}), O7′–H (pK_{a2}), and O6′–H (pK_{a3}) bonds (Fig. 2); the pK_{a1} values of **CQAs** were obtained from a previous study,[66] while the pK_{a2} and pK_{a3} values were computed according to the previous study.[30] The data are displayed in Fig. 3 and Table 1.

The pK_{a1} values for **3CQA** and **5CQA** are 3.95, while those for **4CQA** are 4.14 (Table 1). The range of pK_{a2} values is 7.97 to 8.22, while the range of pK_{a3} values is 12.27 to 12.59. The calculated pK_a values of **5CQA** ($pK_{a2} = 8.22$ and $pK_{a3} = 12.27$) closely align with the experimental results ($pK_{a2} = 8.21$ and $pK_{a3} = 12.5$),[67] providing evidence for the accuracy and validity of the computational approach. The mole fractions $f(H_2A^-)$ and $f(HA^{2-})$ range between 0.788 and 0.868 and between 0.131 and 0.212, respectively, while the H_3A and A^{3-} phases are not present in water at pH = 7.40. Therefore, the **CQAs** exist in both anionic and dianionic states in water with a pH of 7.4. These two states were examined in the subsequent investigation.

3.2.2. The kinetics of the reaction of CQAs with HOO$^{\bullet}$ radical in the physiological environments. The kinetics of the reactions between **CQAs** and HOO$^{\bullet}$ in the aqueous solution were

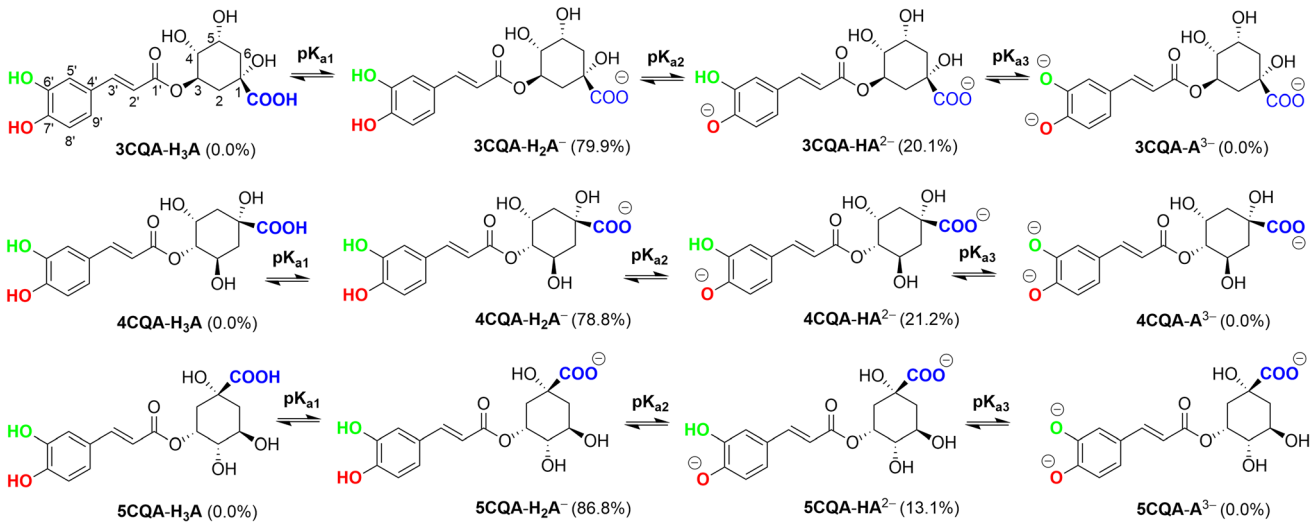

Fig. 3 The deprotonation of **CQAs** in water under pH = 7.40.

Table 1 Calculated pK_a and f

Comp.	Group	pK_a		f (pH = 7.40)[c]	
3CQA	COOH	1	3.95[a]	H_3A	0.000
	O6′–H	2	8.00[b]	H_2A^-	0.799
	O7′–H	3	12.59[b]	HA^{2-}	0.201
				A^{3-}	0.000
4CQA	COOH	1	4.14[a]	H_3A	0.000
	O6′–H	2	7.97[b]	H_2A^-	0.788
	O7′–H	3	12.52[b]	HA^{2-}	0.212
				A^{3-}	0.000
5CQA	COOH	1	3.95[a]	H_3A	0.000
	O6′–H	2	8.22[b]	H_2A^-	0.868
	O7′–H	3	12.27[b]	HA^{2-}	0.131
				A^{3-}	0.000

[a] Ref. 66. [b] Calculated in this work. [c] f Molar fraction.

investigated for all states, using the methodology employed in earlier research on phenolic compounds. The competitive FHT reaction was utilized to evaluate the kinetics for neutral states, while the SET reaction was employed for anion states.[25,31,35] Using eqn (2) and (3), the total rate constants of the states (k_{total}) were determined, whereas eqn (4) was used to derive the rate constant containing the molar fraction (k_f). Fig. 4 depicts the optimized transition structures (TS), data are in Table 2.

Lipid environment:

$$k_{total} = k_{app}(\text{FHT(O6′–H)-neutral}) + k_{app}(\text{FHT(O7′–H)-neutral}) \quad (2)$$

Water at physiological pH:

$$k_{total} = k_f(\text{SET-HA}^-) + k_f(\text{FHT(O6′–H)-HA}^-) + k_f(\text{FHT(O7′–H)-HA}^-) + k_f(\text{SET-A}^{2-}) + k_f(\text{FHT(O6′–H)-A}^{2-}) \quad (3)$$

$$k_f = k_{app} \cdot f \quad (4)$$

As shown in Table 2, the calculations suggest that **CQAs** can be potent HOO˙ scavengers in the nonpolar environment, with $k_{total} = 1.09 \times 10^4$–$1.93 \times 10^4$ M^{-1} s^{-1}. The rate constant for the reaction between **5CQA** and HOO˙ was found to be the highest, whereas the reaction between **3CQA** and HOO˙ exhibited the lowest rate constant. Based on the calculated data, the HOO˙ radical trapping ability of **CQAs** in the lipid medium can be ranked as follows: **5CQA** > **4CQA** > **3CQA**. Thus, the activity of **CQAs** in the nonpolar medium is comparable to reference antioxidants including ascorbic acid ($k = 5.71 \times 10^3$ M^{-1} s^{-1}),[40] resveratrol ($k = 1.31 \times 10^4$ M^{-1} s^{-1}),[64] and Trolox ($k = 3.40 \times 10^3$ M^{-1} s^{-1}).[68]

In water at pH = 7.40, the FHT mechanism of the neighboring hydroxyl group (O6′–H) of the dianion states determined the HOO˙ radical scavenging activity of the **CQAs** (Γ = 93.2–95.2%), while the SET reaction of these species contributed approximately 4.8–6.8% to the k_{total}. It should be noted that the tunneling corrections (κ) had a negligible impact on the H-abstraction rate constant of the dianion state, the substantial imaginary frequencies ($\nu > 3000$ cm^{-1}) of these transition states notwithstanding. This suggests that the remarkably swift reaction rates are caused solely by the excessively low Gibb activation energy ($\Delta G^{\neq}$ = 1.0–5.4 kcal mol^{-1}) ($k_{TST} \approx k_D$, where k_D denotes the diffusion rate). The HOO˙ radical scavenging activity of the **CQAs** was not influenced by the monoanion states, despite the fact these states exist about 13.1% to 21.2% (Table 1) of the **CQAs** in water at pH = 7.4. All compounds exhibit outstanding HOO˙ antiradical activity with $k_{total} \approx 10^8$ M^{-1} s^{-1}. **4CQA** had the maximum activity with $k_{total} = 5.32 \times 10^8$ M^{-1} s^{-1} that is approximately 4.19 and 1.05 times faster than **5CQA** and **3CQA**, respectively. In water at pH = 7.4, the radical trapping activity of **CQAs** against HOO˙ is ranked as follows: **4CQA** > **5CQA** > **3CQA**. In water at physiological pH, the **CQAs** demonstrated $\approx 10^4$ times greater HOO˙ radical scavenging ability than in the nonpolar environment. In water, **CQAs** have greater HOO˙ antiradical capacity than Trolox ($k = 8.96 \times 10^4$ M^{-1} s^{-1}),[68] resveratrol ($k = 5.62 \times 10^7$ M^{-1} s^{-1}),[64] and ascorbic acid ($k = 9.97 \times 10^7$ M^{-1} s^{-1}),[40] but the fairly similar

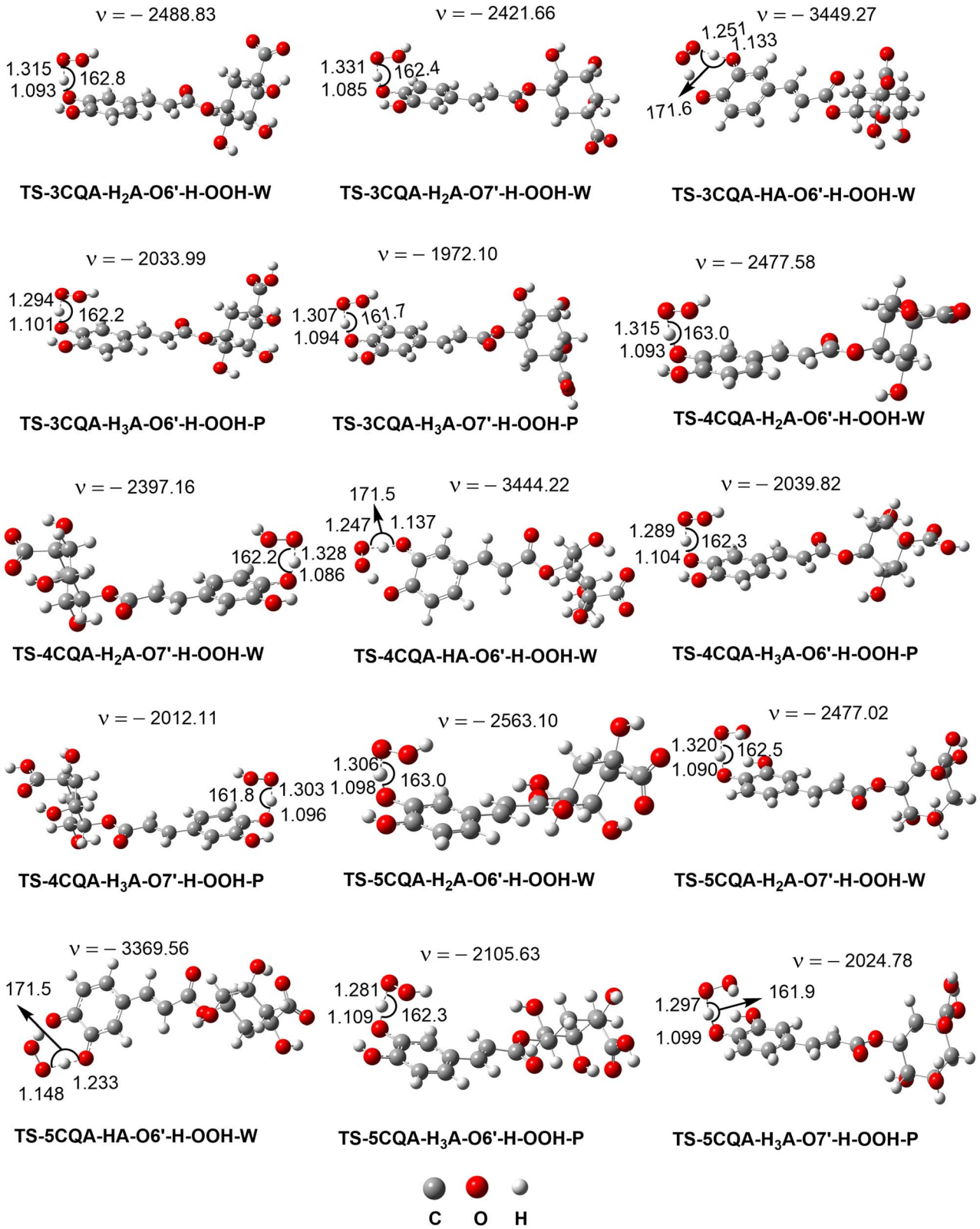

Fig. 4 The FHT TS structures of the HOO˙ + **CQAs** reactions (W: water; P: pentyl ethanoate).

activity to caffeic acid ($k = 2.69 \times 10^8\ M^{-1}\ s^{-1}$), ferulic acid ($k = 3.36 \times 10^8\ M^{-1}\ s^{-1}$) and dihydrocaffeic acid ($k = 1.04 \times 10^8\ M^{-1}\ s^{-1}$).[63] Consequently, **CQAs** are promising natural antioxidants.

According to the information provided above, the removal of a hydrogen atom from the neighboring hydroxyl group (O6′–H bond) of the dianion states is responsible for the

Table 2 Computed $\Delta G^{\neq}$ (kcal mol^{-1}) Γ (%), k_{app}, k_f, and $k_{overall}$ (M^{-1} s^{-1}) of the **CQAs** + HOO$^{\bullet}$ reactions in the studied media

			Pentyl ethanoate			Water					
Comp.	Mechanisms		$\Delta G^{\neq}$	k_{app}	Γ	States	$\Delta G^{\neq}$	k_{app}	F	k_f	Γ
3CQA	SET					H_2A^-	34.3	15.9	0.799	3.84×10^{-13}	0.0
						HA^{2-}	6.4	1.20×10^{8}	0.201	2.41×10^{7}	4.8
	FHT	O6′–H	15.3	6.30×10^{3}	57.8	H_2A^-	15.9	4.80×10^{3}	0.799	3.84×10^{3}	0.0
		O7′–H	15.2	4.60×10^{3}	42.2		16.6	1.00×10^{3}	0.799	7.99×10^{2}	0.0
		O6′–H (HA^{2-})				HA^{2-}	1.0	2.40×10^{9}	0.201	4.82×10^{8}	95.2
	k_{total}			$\mathbf{1.09 \times 10^{4}}$						$\mathbf{5.07 \times 10^{8}}$	
4CQA	SET					H_2A^-	32.3	17.2	0.788	1.10×10^{-8}	0.0
						HA^{2-}	6.4	1.30×10^{8}	0.212	2.76×10^{7}	5.2
	FHT	O6′–H	14.9	8.00×10^{2}	4.8	H_2A^-	16.2	2.10×10^{3}	0.788	1.65×10^{3}	0.0
		O7′–H	14.6	1.60×10^{4}	95.2		16.1	4.70×10^{3}	0.788	3.70×10^{3}	0.0
		O6′–H (HA^{2-})				HA^{2-}	1.8	2.38×10^{9}	0.212	5.05×10^{8}	94.8
	k_{total}			$\mathbf{1.68 \times 10^{4}}$						$\mathbf{5.32 \times 10^{8}}$	
5CQA	SET					H_2A^-	38.2	15.1	0.869	5.56×10^{-16}	0.0
						HA^{2-}	6.8	6.60×10^{7}	0.131	8.65×10^{6}	6.8
	FHT	O6′–H	15.3	9.50×10^{3}	49.2	H_2A^-	18.0	2.40×10^{2}	0.869	2.09×10^{2}	0.0
		O7′–H	15.0	9.80×10^{3}	50.8		17.5	3.10×10^{2}	0.869	2.69×10^{2}	0.0
		O6′–H (HA^{2-})				HA^{2-}	5.4	9.00×10^{8}	0.131	1.18×10^{8}	93.2
	k_{total}			$\mathbf{1.93 \times 10^{4}}$						$\mathbf{1.27 \times 10^{8}}$	

scavenging activity of **CQAs** in water at a pH level that is characteristic of physiological conditions. In this section, AIM analysis was employed to examine the structural characteristics of the transition states (TSs) pertaining to the O6′–H bond. The findings are displayed in Table S3, ESI,† and Fig. 5. The analysis of the AIM data reveals that the stability of the TSs-DIANION-O6′-H-OOH species can be attributed to intermolecular interactions occurring at certain sites, namely O6′⋯H41, O43⋯H41, O7′⋯H42, and PCR(O6′–H41–O43–O44–H42–O7′–C7′–C6′) (Fig. 5), whereas the stability of TSs-ANION-O6′–H–OOH is given by the intramolecular hydrogen bonding at H41⋯O6′, H41⋯O44 and O45⋯C6′ and at PCR(C6′–O6′–H41–O44–O45). The

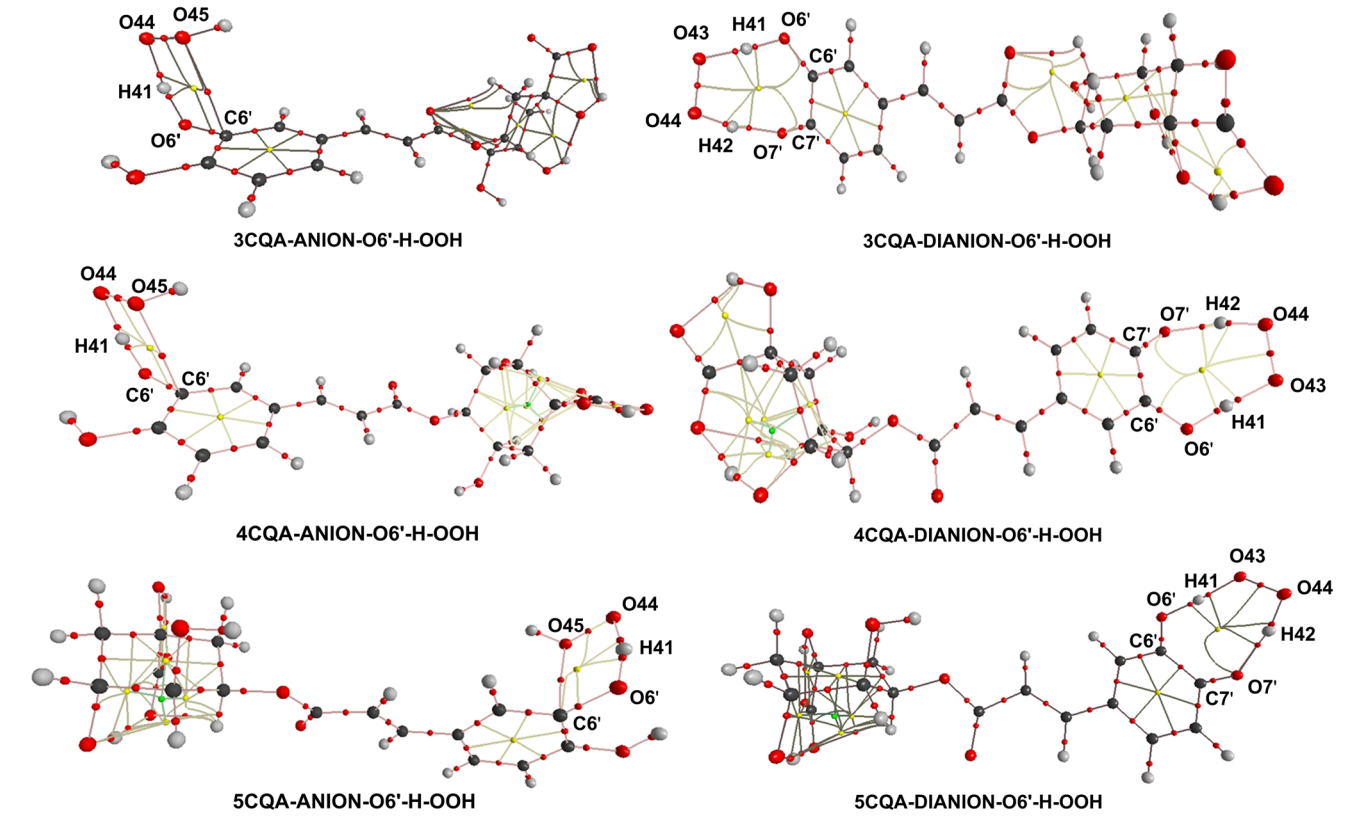

Fig. 5 AIM topological structures of the FHT TSs of the O6′–H bond of the anionic and dianionic states. The bond critical points (BCPs) are represented by red spheres, while the ring critical points (RCPs) are represented by yellow spheres.

formation of an intramolecular hydrogen bond between O7′ and H42 in the TSs-DIANION-O6′-H-OOH results in the creation of an 8-atom ring, which includes O6′–H41–O43–O44–H42–O7′–C7′–C6′ (Fig. 5). The electron density between O7′ and H42 exhibits characteristics of partial covalent bonding, as evidenced by $\nabla^2\rho(r) > 0$, $G(r)/|V(r)| \leq 1$ and $H(r) < 0$.[69,70] This electron density significantly contributes to the stability of the transition state, as revealed by the substantial negative values of E_{HD} (−26.9 to −27.9 kcal mol^{-1}). Thus, the total E_{HB} of TSs-DIANION-O6′–H–OOH (E_{HB} = −211.0 to −212.9 kcal mol^{-1}) is about 1.13 times lower than those of TSs-ANION-O6′–H–OOH (E_{HB} = −184.6 to −186.7 kcal mol^{-1}, respectively). This underpins the increased stability of TSs-DIANION-O6′–H–OOH and consequently the decreased $\Delta G^{\neq}$ values ($\Delta G^{\neq}$ = 1.0–5.4 kcal mol^{-1}) in comparison with the remaining TSs.

3.3. The effect of pH values on the reactions of CQAs with HOO˙ in water

The impact of solution pH on the rate constants was also evaluated. Eqn (5)–(8) were employed in the computation of several key parameters, namely the rate constant (k), the rate constant specific to each protonation state (k_{state}), the total rate constant (k_{total}), and the overall rate constant ($k_{overall}$). The outcomes are displayed in Fig. 6 and Table 3.

$$k = k_{app}(\text{SET}) + \sum k_{app}(\text{FHT}) \quad (5)$$

$$k_{state} = k \cdot f(\text{CQA}) \quad (6)$$

$$k_{total} = \sum k_{state} \quad (7)$$

$$k_{overall} = f(\text{HOO}^{\bullet}) \cdot k_{total} \quad (8)$$

The log(k_{total}) for the total rate constant (Fig. 6a) did not change below pH 4.7, however, it increased significantly between pH = 4.8 and 8.3 by 4–6 units and afterward grew progressively until pH 14. The sudden increase in the log(k_{total}) figures at pH = 4.8 and 8.3 is due to the appearance of HA^{2-} states and thus the onset of rapid SET processes. In acidic media (pH < 4.7), the reactions between **CQAs** and HOO˙ are sluggish because the majority of the **CQAs** exist in the H_3A states (neutral states), acting *via* a slow FHT reaction.

It was demonstrated that pK_a(HOO˙) is 4.80, and thus the f(HOO˙) value is zero at pH > 9.1. Since only pH levels below 9.1 had any impact on the $k_{overall}$ values of reactions between **CQAs** and HOO˙, only these were looked at (Fig. 6b). It was found that as the pH levels rose, the $k_{overall}$ changed. Most of the studied acids showed a rise in log($k_{overall}$) at pH 4; after a brief fall, the log($k_{overall}$) significantly rose at pH = 4.7–6.5, before decreasing

Table 3 Calculated $\Delta G^{\neq}$ (kcal mol^{-1}), k_{app} and k (M^{-1} s^{-1}) of the **CQAs** + HOO˙ reactions in the water

Comp.	States	Mechanisms		$\Delta G^{\neq}$	k_{app}	k
3CQA	H_3A	FHT	O6′–H	17.4	5.80×10^{2}	1.86×10^{3}
			O7′–H	17.1	1.28×10^{3}	
	H_2A^-	SET		34.3	4.80×10^{-13}	5.80×10^{3}
		FHT	O6′–H	15.9	4.80×10^{3}	
			O7′–H	16.6	1.00×10^{3}	
	HA^{2-}	SET		6.4	1.20×10^{8}	2.52×10^{9}
		FHT	O6′–H	1.0	2.40×10^{9}	
	A^{3-}	SET		0.0	8.10×10^{9}	8.10×10^{9}
4CQA	H_3A	FHT	O6′–H	16.3	5.00×10^{1}	2.15×10^{3}
			O7′–H	16.6	2.01×10^{3}	
	H_2A^-	SET		32.3	1.40×10^{-11}	6.80×10^{3}
		FHT	O6′–H	16.2	2.10×10^{3}	
			O7′–H	16.1	4.70×10^{3}	
	HA^{2-}	SET		6.4	1.30×10^{8}	2.51×10^{9}
		FHT	O6′–H	1.8	2.38×10^{9}	
	A^{3-}	SET		0.0	8.10×10^{9}	8.10×10^{9}
5CQA	H_3A	FHT	O6′–H	17.0	1.80×10^{3}	2.23×10^{3}
			O7′–H	18.0	4.30×10^{2}	
	H_2A^-	SET		38.2	6.40×10^{-16}	5.50×10^{2}
		FHT	O6′–H	18.0	2.40×10^{2}	
			O7′–H	17.5	3.10×10^{2}	
	HA^{2-}	SET		6.8	6.60×10^{7}	9.66×10^{8}
		FHT	O6′–H	5.4	9.00×10^{8}	
	A^{3-}	SET		0.0	8.30×10^{9}	8.30×10^{9}

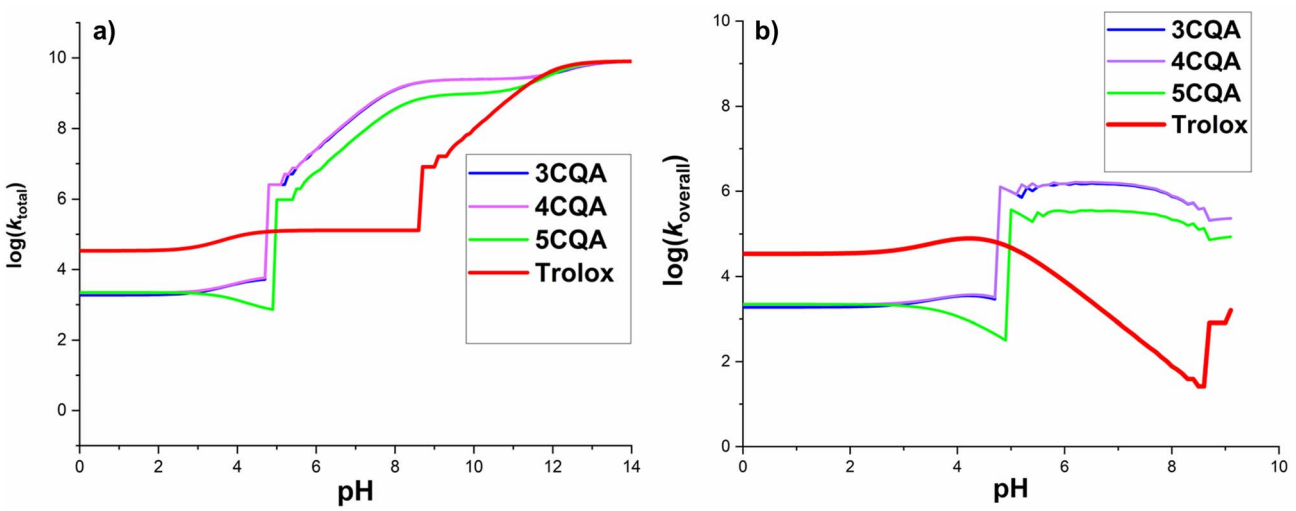

Fig. 6 Calculated log(k_{total}) (a) and log($k_{overall}$) (b) at 298.15 K, in the **CQAs** + HOO˙ in water as a function of pH values.

once again. For this range, $k_{overall}$ was 0 because $f(HOO^{\bullet}) = 0$ at pH > 9.2 (Fig. 6b).

In terms of the **CQAs**, the exhibition was fairly similar to the HOO$^{\bullet}$ antiradical activity at pH < 3, however at the rest pH values, **5CQA** reacted with the HOO$^{\bullet}$ lower than **3CQA** or **4CQA**. It is important to notice that the **3CQA** acid had a fairly similar HOO$^{\bullet}$ radical scavenging activity to **4CQA** in all of the studied pH levels. Compared with typical antioxidant-Trolox, at pH 4.7, **CQAs** had less HOO$^{\bullet}$ radical scavenging activity than Trolox; nevertheless, at pH > 5.0, these acids reacted with the HOO$^{\bullet}$ more quickly than the standard. According to the calculated data, in the pH range of 5.0–8.6, the **CQAs** had the highest HOO$^{\bullet}$ antiradical activity ($\log(k_{overall}) = 5.1$–6.2). It was found that the calculated rate constant for the **5CQA** + HOO$^{\bullet}$ reaction ($k_{overall}$(calculation) $= 3.10 \times 10^5$ M^{-1} s^{-1}) exhibit a high level of consistence with the empirical observations ($k_{exp} = 1.28 \times 10^5$ M^{-1} s^{-1}, pH = 7.5).[17] Therefore, the computed kinetic values are fairly accurate.

4. Conclusion

DFT calculations were performed to examine the effectiveness of monocaffeoylquinic acids in scavenging hydroperoxyl radicals. In water at physiological pH, the **CQAs** demonstrated ≈ 10^4 times (k(water, pH = 7.4) = 1.27–5.32 $\times 10^8$ M^{-1} s^{-1}) greater HOO$^{\bullet}$ radical-trapping activity than in the nonpolar environment (k(lipid) = 1.09–1.93 $\times 10^4$ M^{-1} s^{-1}). The FHT reaction of the neighboring hydroxyl group (O6′–H) of the dianion states determined the activity in the aqueous solution ($\Gamma = 93.2$–95.2%), while the SET mechanism of these states contributed 4.8–6.8% to the total rate constants. It is significant that the computed rate constant of the HOO$^{\bullet}$ radical-trapping activity in water at pH 7.5 agrees favorably with experimental findings ($k_{calculated}/k_{experimental} = 2.4$), supporting the computational method. **CQAs** exhibited similar HOO$^{\bullet}$ antiradical activities at pH < 3, however at higher pH values, **5CQA** reaction with HOO$^{\bullet}$ was slower than that of **3CQA** or **4CQA**. It was also found that **CQAs** had less HOO$^{\bullet}$ radical scavenging activity than Trolox at pH 4.7 while at pH > 5.0 **CQAs** are better radical scavengers than the reference. The **CQAs** had the highest HOO$^{\bullet}$ antiradical activity at pH = 5.0–8.6. Thus, in the physiological environments, the HOO$^{\bullet}$ antiradical ability of **CQAs** is generally better than the reference antioxidants resveratrol, ascorbic acid, and Trolox.

Conflicts of interest

There are no conflicts to declare.

Acknowledgements

The research is funded by the Vietnam National Foundation for Science and Technology Development (NAFOSTED) under grant number 104.06-2021.14.

References

1 A. Alcázar Magaña, N. Kamimura, A. Soumyanath, J. F. Stevens and C. S. Maier, *Plant J.*, 2021, **107**, 1299–1319.
2 S. Moyo, J. Serem, M. Bester, V. Mavumengwana and E. Kayitesi, *Food Chem.*, 2020, **311**, 126023.
3 C. Ma, K. Dastmalchi, B. D. Whitaker and E. J. Kennelly, *J. Agric. Food Chem.*, 2011, **59**, 9645–9651.
4 Y. Nakajima, M. Shimazawa, S. Mishima and H. Hara, *Life Sci.*, 2007, **80**, 370–377.
5 X. Li, K. Li, H. Xie, Y. Xie, Y. Li, X. Zhao, X. Jiang and D. Chen, *Molecules*, 2018, **23**, 222.
6 W. Liu, J. Li, X. Zhang, Y. Zu, Y. Yang, W. Liu, Z. Xu, H. Gao, X. Sun and X. Jiang, *J. Agric. Food Chem.*, 2020, **68**, 10489–10516.
7 M. Naveed, V. Hejazi, M. Abbas, A. A. Kamboh, G. J. Khan, M. Shumzaid, F. Ahmad, D. Babazadeh, X. FangFang and F. Modarresi-Ghazani, *Biomed. Pharmacother.*, 2018, **97**, 67–74.
8 O. Bender and A. Atalay, in *Cancer*, Elsevier, 2021, pp. 311–321, DOI: 10.1016/B978-0-12-819547-5.
9 Y. S. Hamed, M. Abdin, G. Chen, H. M. S. Akhtar and X. Zeng, *Int. J. Food Sci. Technol.*, 2020, **55**, 3082–3090.
10 F. K. Nzekoue, S. Angeloni, L. Navarini, C. Angeloni, M. Freschi, S. Hrelia, L. A. Vitali, G. Sagratini, S. Vittori and G. Caprioli, *Food Res. Int.*, 2020, **133**, 109128.
11 M. Carvalho, B. M. Silva, R. Silva, P. Valentao, P. B. Andrade and M. L. Bastos, *J. Agric. Food Chem.*, 2010, **58**, 3366–3370.
12 N. Benchikha, M. Messaoudi, I. Larkem, H. Ouakouak, A. Rebiai, S. Boubekeur, M. A. Ferhat, A. Benarfa, S. Begaa and M. Benmohamed, *Life*, 2022, **12**, 1579.
13 N. Liang and D. D. Kitts, *Nutrients*, 2015, **8**, 16.
14 R. Socodato, C. C. Portugal, T. Canedo, I. Domith, N. A. Oliveira, R. Paes-de-Carvalho, J. B. Relvas and M. Cossenza, *Free Radical Biol. Med.*, 2015, **79**, 45–55.
15 D. Woźniak, I. Nawrot-Hadzik, W. Kozłowska, S. Ślusarczyk and A. Matkowski, *Caffeoylquinic Acids*, 2021.
16 J.-G. Xu, Q.-P. Hu and Y. Liu, *J. Agric. Food Chem.*, 2012, **60**, 11625–11630.
17 Y. Kono, K. Kobayashi, S. Tagawa, K. Adachi, A. Ueda, Y. Sawa and H. Shibata, *Biochim. Biophys. Acta, Gen. Subj.*, 1997, **1335**, 335–342.
18 J. Tošović, S. Marković, J. M. D. Marković, M. Mojović and D. Milenković, *Food Chem.*, 2017, **237**, 390–398.
19 J. Tošović and S. Marković, *Food Chem.*, 2019, **278**, 469–475.
20 S. Marković and J. Tošović, *Food Chem.*, 2016, **210**, 585–592.
21 J. G. Uranga, N. S. Podio, D. A. Wunderlin and A. N. Santiago, *ChemistrySelect*, 2016, **1**, 4113–4120.
22 S. Dobrev and S. Angelova, *Bulg. Chem. Commun.*, 2020, **52**, 48–53.
23 O. K. Yusuff, M. A. O. Abdul Raheem, A. A. Mukadam and R. O. Sulaimon, *ACS Omega*, 2019, **4**, 13671–13680.
24 H. Boulebd, A. Mechler, N. T. Hoa and Q. V. Vo, *New J. Chem.*, 2022, **46**, 7403–7409.
25 N. T. Hoa and Q. V. Vo, *RSC Adv.*, 2022, **12**, 15115–15122.
26 I. I. Junior, M. A. Do Nascimento, R. O. M. A. de Souza, A. Dufour and R. Wojcieszak, *Green Chem.*, 2020, **22**, 5859–5880.
27 D. S. Dimić, D. A. Milenković, E. H. Avdović, Đ. J. Nakarada, J. M. Dimitrić Marković and Z. S. Marković, *J. Chem. Eng.*, 2021, **424**, 130331.
28 D. A. Milenković, D. S. Dimić, E. H. Avdović, A. D. Amić, J. M. Dimitrić Marković and Z. S. Marković, *J. Chem. Eng.*, 2020, **395**, 124971.

29 N. T. Hoa and Q. V. Vo, *Chemosphere*, 2023, **314**, 137682.
30 A. Galano, A. Pérez-González, R. Castañeda-Arriaga, L. Muñoz-Rugeles, G. Mendoza-Sarmiento, A. Romero-Silva, A. Ibarra-Escutia, A. M. Rebollar-Zepeda, J. R. León-Carmona, M. A. Hernández-Olivares and J. R. Alvarez-Idaboy, *J. Chem. Inf. Model.*, 2016, **56**, 1714–1724.
31 Q. V. Vo, N. T. Hoa, N. M. Thong and A. Mechler, *Phytochemistry*, 2021, **192**, 112968.
32 A. S. M. Gonçalves, R. G. Peixe, A. Sato, M. F. Muzitano, R. O. M. A. de Souza, T. de Barros Machado, A. C. F. Amaral, M. R. L. Moura, N. K. Simas and I. C. R. Leal, *Food Res. Int.*, 2015, **70**, 110–117.
33 M. C. Marcondes, A. C. Fernandes, I. Itabaiana Jr, R. O. de Souza, M. Sola-Penna and P. Zancan, *PLoS One*, 2015, **10**, e0130555.
34 M. Carreon-Gonzalez, A. Vivier-Bunge and J. R. Alvarez-Idaboy, *J. Comput. Chem.*, 2019, **40**, 2103–2110.
35 A. Galano and J. Raúl Alvarez-Idaboy, *Int. J. Quantum Chem.*, 2019, **119**, e25665.
36 Y. Zhao, N. E. Schultz and D. G. Truhlar, *J. Chem. Theory Comput.*, 2006, **2**, 364–382.
37 A. Galano and J. R. Alvarez-Idaboy, *J. Comput. Chem.*, 2014, **35**, 2019–2026.
38 Y. Zhao and D. G. Truhlar, *J. Phys. Chem. A*, 2008, **112**, 1095–1099.
39 J. R. l. Alvarez-Idaboy and A. Galano, *J. Phys. Chem. B*, 2012, **116**, 9316–9325.
40 A. Galano and J. R. Alvarez-Idaboy, *J. Comput. Chem.*, 2013, **34**, 2430–2445.
41 Q. V. Vo, M. V. Bay, P. C. Nam, D. T. Quang, M. Flavel, N. T. Hoa and A. Mechler, *J. Org. Chem.*, 2020, **85**, 15514–15520.
42 Q. V. Vo, N. T. Hoa and A. Mechler, *Polym. Degrad. Stab.*, 2021, **185**, 109483.
43 A. Galano, *J. Mex. Chem. Soc.*, 2015, **59**, 231–262.
44 M. G. Evans and M. Polanyi, *Trans. Faraday Soc.*, 1935, **31**, 875–894.
45 H. Eyring, *J. Chem. Phys.*, 1935, **3**, 107–115.
46 D. G. Truhlar, W. L. Hase and J. T. Hynes, *J. Phys. Chem.*, 1983, **87**, 2664–2682.
47 T. Furuncuoglu, I. Ugur, I. Degirmenci and V. Aviyente, *Macromolecules*, 2010, **43**, 1823–1835.
48 E. Vélez, J. Quijano, R. Notario, E. Pabón, J. Murillo, J. Leal, E. Zapata and G. Alarcón, *J. Phys. Org. Chem.*, 2009, **22**, 971–977.
49 E. Pollak and P. Pechukas, *J. Am. Chem. Soc.*, 1978, **100**, 2984–2991.
50 A. Fernández-Ramos, B. A. Ellingson, R. Meana-Pañeda, J. M. Marques and D. G. Truhlar, *Theor. Chem. Acc.*, 2007, **118**, 813–826.
51 C. Eckart, *Phys. Rev.*, 1930, **35**, 1303.
52 M. J. Frisch, G. W. Trucks, H. B. Schlegel, G. E. Scuseria, M. A. Robb, J. R. Cheeseman, G. Scalmani, V. Barone, B. Mennucci, G. A. Petersson, H. Nakatsuji, M. Caricato, X. Li, H. P. Hratchian, A. F. Izmaylov, G. Z. J. Bloino, J. L. Sonnenberg, M. Hada, M. Ehara, K. Toyota, R. Fukuda, J. Hasegawa, M. Ishida, T. Nakajima, Y. Honda, O. Kitao, H. Nakai, T. Vreven, J. A. Montgomery, J. E. P. Jr., F. Ogliaro, M. Bearpark, J. J. Heyd, E. Brothers, K. N. Kudin, V. N. Staroverov, T. Keith, R. Kobayashi, J. Normand, K. Raghavachari, A. Rendell, J. C. Burant, S. S. Iyengar, J. Tomasi, M. Cossi, N. Rega, J. M. Millam, M. Klene, J. E. Knox, J. B. Cross, V. Bakken, C. Adamo, J. Jaramillo, R. Gomperts, R. E. Stratmann, O. Yazyev, A. J. Austin, R. Cammi, C. Pomelli, J. W. Ochterski, R. L. Martin, K. Morokuma, V. G. Zakrzewski, G. A. Voth, P. Salvador, J. J. Dannenberg, S. Dapprich, A. D. Daniels, O. Farkas, J. B. Foresman, J. V. Ortiz, J. Cioslowski and D. J. Fox, Gaussian, Inc., Wallingford CT, 2016.
53 E. Dzib, J. L. Cabellos, F. Ortíz-Chi, S. Pan, A. Galano and G. Merino, *Int. J. Quantum Chem.*, 2019, **119**, e25686.
54 E. Dzib, J. L. Cabellos, F. Ortiz-Chi, S. Pan, A. Galano and G. Merino, *Eyringpy 1.0.2*, Cinvestav, Mérida, Yucatán, 2018.
55 R. F. Bader, *Chem. Rev.*, 1991, **91**, 893–928.
56 F. Biegler-König, *AIM 2000*, University of Applied Sciences, Bielefeld, Germany, 2000.
57 W. Hehre, J. Yu, P. Klunzinger and L. Lou, *Spartan Software*, Wavefunction Inc, Irvine, 2000.
58 A. Galano and J. R. Alvarez-Idaboy, *RSC Adv.*, 2011, **1**, 1763–1771.
59 Q. V. Vo, N. M. Tam, M. Van Bay and A. Mechler, *Chem. Phys. Lett.*, 2020, **739**, 137004.
60 K. U. Ingold and D. A. Pratt, *Chem. Rev.*, 2014, **114**, 9022–9046.
61 A. Galano, G. Mazzone, R. Alvarez-Diduk, T. Marino, J. R. Alvarez-Idaboy and N. Russo, *Annu. Rev. Food Sci. Technol.*, 2016, **7**, 335–352.
62 D. Dimić, D. Milenković, J. D. Marković and Z. Marković, *Phys. Chem. Chem. Phys.*, 2017, **19**, 12970–12980.
63 J. R. León-Carmona, J. R. Alvarez-Idaboy and A. Galano, *Phys. Chem. Chem. Phys.*, 2012, **14**, 12534–12543.
64 M. Cordova-Gomez, A. Galano and J. R. Alvarez-Idaboy, *RSC Adv.*, 2013, **3**, 20209–20218.
65 C. Iuga, J. R. l. Alvarez-Idaboy and N. Russo, *J. Org. Chem.*, 2012, **77**, 3868–3877.
66 J. Wang, D. Lu, Q. Sun, H. Zhao, X. Ling and P. Ouyang, *Chem. Eng. Sci.*, 2012, **78**, 53–62.
67 T. Kiss, G. Nagy, M. Pécsi, H. Kozlowski, G. Micera and L. S. Erre, *Polyhedron*, 1989, **8**, 2345–2349.
68 M. E. Alberto, N. Russo, A. Grand and A. Galano, *Phys. Chem. Chem. Phys.*, 2013, **15**, 4642–4650.
69 M. Ziółkowski, S. J. Grabowski and J. Leszczynski, *J. Phys. Chem. A*, 2006, **110**, 6514–6521.
70 I. Rozas, I. Alkorta and J. Elguero, *J. Am. Chem. Soc.*, 2000, **122**, 11154–11161.